# An accounting of C-based trace gas release during abiotic plant litter degradation

HANNA LEE*, THOM RAHN† and HEATHER THROOP*

*Department of Biology, New Mexico State University, Las Cruces, NM 88003, USA, †Earth and Environmental Sciences Division, Los Alamos National Laboratory, Los Alamos, NM 87545, USA

## Abstract

Recent studies showed that photochemical breakdown (photodegradation) of plant material accounts for a substantial portion of litter decomposition and subsequent trace gas release in ecosystems under high radiative load and low precipitation. In the absence of solar radiation, thermal degradation may also cause trace gas release at temperatures below the ignition point. These observations suggest that the abiotic processes of photodegradation and thermal degradation of plant litter may be important in understanding global trace gas budgets. In a laboratory incubation study, we performed a simultaneous carbon (C) accounting of $CO_2$, $CO$, and $CH_4$ produced as a byproduct of photodegradation and thermal degradation of six different plant litter types that varied in chemical composition. The patterns of trace gas release during photodegradation and thermal degradation differed considerably across the six plant materials, suggesting that chemical composition of litter may influence the rates of abiotic degradation. There was a strong positive correlation between the rates of trace gas release during photodegradation and temperature. A significant portion of trace gases were produced during low temperature (< 100 °C) thermal degradation of litter in the absence of solar radiation, which was also positively correlated to temperature. In addition, both thermal degradation and photodegradation occurred in the absence of $O_2$. This indicates that the mechanism formerly accepted as photo-oxidation may only be one of several photodegradation processes. We speculate that the direct breakdown of chemical groups such as carboxyl, carbonyl, and methoxyl groups may result in $CO_2$, $CO$, and $CH_4$ release. We suggest that the combined processes of thermal and photodegradation of litter may be a previously under accounted source of C-based trace gases from terrestrial systems.

*Keywords:* CH4, CO, CO2, litter decomposition, photodegradation, thermal degradation

## Introduction

Decomposition of plant litter and soil organic matter is a key biogeochemical process that controls the rates and pathways of global C and nutrient cycling. There are nearly 200 Pg C (1 Pg = $10^{15}$ g) of plant-derived litter in the global terrestrial C pool (DeFries & Townshend, 1994; Matthews, 1997). Litter decomposes to become soil organic matter, which globally accounts for 2000 Pg C in the top 3 m of the soil (Jobbagy & Jackson, 2000). Decomposition of terrestrial litter and soil organic matter releases approximately 10 times more C to the atmosphere annually than does fossil fuel burning (Gholz et al., 2000; IPCC, 2007), illustrating the potential importance of litter decomposition to climate change.

Recent studies suggest that photodegradation of plant litter and organic material can circumvent micro-bial decomposition in arid and semi-arid ecosystems, where microbial decomposition is often limited (Austin & Vivanco, 2006; Rutledge et al., 2010). Photodegradation has been linked to significant litter mass loss after litter exposure to manipulated solar radiation and ultraviolet (UV) radiation (Austin & Vivanco, 2006; Day et al., 2007; Henry et al., 2008). Several other studies have identified and quantified a number of C-based gaseous products during photodegradation of plant litter and organic matter: $CO_2$ (Brandt et al., 2009; Rutledge et al., 2010), $CO$ (Tarr et al., 1995; Schade et al., 1999), and $CH_4$ (Vigano et al., 2008, 2009; Bruhn et al., 2009). Although evidence to date clearly supports that photodegradation can play a large role in litter decomposition in arid and semi-arid ecosystems (Austin, 2011), other studies suggest that abiotic factors can be more important than photodegradation, even in high solar radiation environments (Throop & Archer, 2007, 2009; Uselman et al., 2011). Therefore, the overall importance of photodegradation on litter decomposition remains unresolved.

Differences in the complexity and structure of chemical constituents (i.e., sugar, cellulose, protein, lignin,

Correspondence: Hanna Lee, Climate and Global Dynamics Division, National Center for Atmospheric Research, Boulder, CO 80307, USA, tel. + 1 303 497 1738, fax + 1 303 497 1348, e-mail: hannal@ucar.edu

*etc.*) present in plant tissues suggests that tissues may vary in susceptibility to photodegradation. The chemical bonds forming these compounds differ in bond dissociation energy (e.g., typically a C–C bond requires 348 kJ mol$^{-1}$ to break and a C=C bond requires 614 kJ mol$^{-1}$ to break) and certain C-based chemical groups have higher radiation absorbance than others, and hence, the potential to be more susceptible to photodegradation. In particular, the complex molecular structure of lignin appears to result in greater radiation absorbance and subsequent photodegradation than less complex compounds such as cellulose (Pancotto *et al.*, 2005; Luo *et al.*, 2009; Austin & Ballare, 2010). The absolute and relative rates of trace gas release would not only depend on energy absorbance of the chemical bonds, but also on the abundance of these chemical bonds present within the organic material. This suggests that plant materials may have highly species- and tissue-specific photodegradation rates depending on their chemical composition.

Several studies have suggested that the rate of photodegradation is correlated to environmental factors (i.e., UV radiation intensity, precipitation, and temperature). Across the wide spectrum of solar radiation wavelengths reaching the Earth's surface, UV-B (280–315 nm) appears to be the most effective in photodegradation of plant litter (Rozema *et al.*, 1997; Brandt *et al.*, 2009; Bruhn *et al.*, 2009). However, both UV-A (315–400 nm) and visible light (380–750 nm) are also involved in breakdown of chemical bonds (Austin & Vivanco, 2006; Austin & Ballare, 2010). In addition, the effects of UV radiation on the rate of litter photodegradation was greatest in drier regions compared with wetter regions that receive considerable amount of precipitation, where photodegradation did not significantly influence litter decomposition (Brandt *et al.*, 2007, 2010). Although the rate of litter photodegradation and trace gas production may be sensitive to temperature (Austin & Vivanco, 2006; Vigano *et al.*, 2008; Bruhn *et al.*, 2009), there has been limited study of the relationship between temperature and litter photodegradation in detail. High surface temperatures along with high incident solar radiation may serve as important drivers of abiotic degradation pathways in arid and semi-arid systems (Austin & Vivanco, 2006; McCalley & Sparks, 2009), where surface temperatures frequently exceed 50 °C in summer months (Rosentreter & Belnap, 2003). Projected global-scale increases in surface temperature and UV radiation (Cheymol & De Backer, 2003; Arola & Koskela, 2004) and decreases in precipitation (IPCC, 2007) suggest that abiotic decomposition pathways may become more important in the future (Caldwell *et al.*, 2007). In addition to the direct influence on abiotic decomposition, these changes are likely to decrease suitable environmental conditions for microbial decomposition.

Several studies have observed small, but significant C-based trace gas release even when the radiation sources were eliminated (Tarr *et al.*, 1995; Vigano *et al.*, 2008), with gas production rate being strongly positively correlated with temperature. Similarly, a study of nitrogen-based gas fluxes conducted in the Mojave Desert showed that high surface temperatures driven by intense solar radiation resulted in the release of NO, $NO_x$, and $NH_3$ from soils (McCalley & Sparks, 2009). These studies suggest that abiotic decomposition may occur not only from photodegradation, but also from thermal degradation of plant litter and soil organic matter occurring at relatively low temperatures (< 100 °C) that are well below the ignition point.

Although previous studies have focused on identification and quantification of trace gas production during photodegradation and thermal degradation, the mechanisms driving this gas production are still unclear. In general, photodegradation processes have been thought to depend on atmospheric $O_2$ (Valentine & Zepp, 1993; Tarr *et al.*, 1995), and are consequently often referred to as photo-oxidation. The requirement for $O_2$ may not be supported; however, as certain studies have suggested that the direct breakdown of chemical groups may occur in the absence of $O_2$ when certain chemical bonds absorb energy. For instance, CO production during photodegradation of organic compounds was attributed to the cleavage of carbonyl groups (Tarr *et al.*, 1995; Schade *et al.*, 1999) and $CH_4$ photoproduction from live and dead plant tissue was attributed to the loss of methoxyl groups that are abundant in lignin and pectin (Keppler *et al.*, 2008; McLeod *et al.*, 2008; Vigano *et al.*, 2008). Together, these putative pathways suggest that dissociation of chemical bonds may occur in the absence of solar radiation if adequate thermal energy is present, and also that photodegradation may occur in the absence of $O_2$. In addition, increased heat energy may act synergistically in combination with radiative energy in the breakdown of chemical bonds, thus the rate of photodegradation would respond positively to temperature.

In this laboratory incubation study, we report a simultaneous C accounting of $CO_2$, CO, and $CH_4$ produced as a byproduct of photodegradation and thermal degradation of plant litter. Understanding the controls over the rates of different trace gas release during abiotic litter decomposition is critical for predicting the impacts of this alternative C cycling pathway on atmospheric chemistry, as gas species differ in their climate forcings (e.g., $CH_4$ has ×25 global warming potential than $CO_2$ on a 100 year time frame; IPCC, 2007). Previous measurements of C-based gas fluxes during

photodegradation of organic compounds have focused on the identification and quantification of individual gas species, and a simultaneous accounting of $CO_2$, CO, and $CH_4$ produced during photodegradation of plant litter has not been reported. In addition, the relative influence of thermal degradation and photodegradation on production of the different C-based trace gases has not been previously documented.

We hypothesized that (1) the rates and ratios of the three C-based gases released during photodegradation would differ with litter chemical composition; (2) low temperature thermal degradation would result in measurable trace gas release in the absence of solar radiation and would be positively related to temperature; (3) the rate of trace gas production during photodegradation and thermal degradation would be enhanced by $O_2$, but there would be detectable gas production in the absence of $O_2$ due to direct breakdown of chemical compounds and (4) that these pathways and processes will have activation energies that fit the Arrhenius form and should be expected to behave in an exponential manner. Lastly, we extended the results from our experimental study to generate rudimentary estimates of the global annual C-based trace gas release from abiotic decomposition of plant litter.

For the purposes of this work, we differentiate two mechanisms that lead to abiotic degradation: thermal degradation and photodegradation of plant material. We define gases produced at various temperatures *in the absence* of solar radiation as a result of low temperature thermal degradation (hereafter 'thermal degradation', < 100 °C) of plant litter. Trace gases produced *in the presence* of solar radiation includes both thermal degradation and photodegradation. Gas production due to photodegradation (i.e., reactions that involve the direct participation of incident solar radiation), therefore, is the difference between the total gas production when exposed to solar radiation and that produced due to thermal degradation. In this study, we define combined effects of thermal degradation and photodegradation as abiotic degradation of plant material.

## Materials and methods

### Experimental design

In a series of controlled laboratory experiments, we exposed six different plant materials to a factorial manipulation of simulated solar radiation (+rad: radiation present, −rad: radiation absent) and temperature (15, 25, 35, 45, and 55 °C) to quantify the patterns of trace gas release during abiotic degradation of plant litter. During these manipulations, we simultaneously quantified the steady state production rates of $CO_2$, CO, and $CH_4$. We subsequently used the plant mate-

rial that exhibited the highest rate of trace gas production (wood sheets from basswood) to quantify the rates of trace gas production in the presence and absence of $O_2$ in combination with solar radiation (+rad and −rad) and temperature (15, 35, and 55 °C).

Experiments were conducted in a quartz chamber that was transparent to over 85% of the radiation generated from the solar radiation simulator across all wavebands. The area of solar radiation exposure was defined by a Viton-core O-ring (53.5 $cm^2$ and 10.5 mL), which was clamped airtight in between the top and bottom halves of the quartz chamber. The area within the O-ring was completely filled with a monolayer of litter material. We standardized the data by surface area of exposure among different litter types instead of mass to maximize the area of exposure and because gas production was sensitive to area of solar radiation exposure rather than mass (e.g., exposing multiple layers of filter paper did not influence the rate of gas production during photodegradation; data not shown). The exposed litter material was exchanged after one full set of temperature and radiation manipulations (temperature increase from 15 to 55 °C and ± rad), although reusing the material did not change the rate of gas production (data not shown; one set of measurements is equivalent to one afternoon exposure of solar radiation). The chamber temperature was controlled using a water bath integrated into the bottom of the chamber and connected to a chiller/heater (ThermoCube 200/300/400, Solid State Cooling Systems, Wappingers Falls, NY, USA). The chamber temperature was continuously monitored with a thermocouple (error range ± 0.5 °C) and radiation influences on chamber temperature (approximately 2 °C) were controlled with the water bath.

Solar radiation was simulated with a 300 W xenon lamp (Model 6258, Oriel Instruments, Newport Corp., Irvine, CA, USA) attached to a lamp housing (Model 66353, Simplicity Arc Source, Oriel Instruments, Newport Corp., Irvine, CA, USA). The xenon lamp, which generated a range of radiation wavelengths (0–2400 nm), was fitted with an atmospheric attenuation filter (Model 81017, Oriel Instruments, Newport Corp., Irvine, CA, USA) to mimic the solar radiation wavelengths that naturally reach the Earth's surface. The filter eliminated short (< 290 nm) and long wavelengths (> 1600 nm) that are naturally filtered out in the atmosphere. As the atmospheric attenuation filter eliminated UV-C (100–280 nm) and the residence time of gases in the chamber was shorter than 10 s, we expect that the effects of $O_3$ generated from the xenon lamp on our results were minimal. However, we did consider the effects of reactive oxidized species (ROS) in our study and discussed the effects of ROS on photodegradation (refer to 'Discussion'). The intensity of radiation varied among wavelengths; UV-B (50 $\mu W\ cm^{-2}$) was generated at a similar intensity as solar radiation, but UV-A was appreciably lower (1 $mW\ cm^{-2}$) than natural incident solar radiation (e.g., measured UV radiation intensity at solar noon during early August on a cloud-free day in northern New Mexico was approximately 55 $\mu W\ cm^{-2}$ for UV-B and 5 $mW\ cm^{-2}$ for UV-A). For −rad measurements, the chamber was covered with aluminum foil to eliminate any radiation from entering the chamber.

## Characteristics of plant materials

We used six different plant-derived materials that varied in chemical and structural composition: four species of plant litter collected from their native habitats in the southwestern US, dried leaflets of velvet mesquite (*Prosopis velutina*), culms and leaves of Indian ricegrass (*Oryzopsis hymenoides*, $C_4$ grass) and little bluestem grass (*Schizachyrium scoparium*, $C_3$ grass), and piñon pine needles (*Pinus edulis*), and two proxies for cellulose and lignin end members, cellulosic filter paper (92% pure cellulose, Whatman 42, GE Healthcare Inc., Piscataway, NJ, USA), and 1/16 inch thick sheets of wood from basswood (*Tilia* sp., high lignin content, National Balsa, Ware, MA, USA). These materials are idealized and may behave differently than what might be found in the field; however, they are good representation of the end members in litter chemistry.

All materials were air dried at 35 °C overnight before use. Filter paper and basswood sheets were precut to fill the entire chamber area, whereas grass material and piñon pine needles were cut to 1 cm lengths to facilitate nonoverlapping arrangement in the chamber. Mesquite leaflets were used without cutting. Due to differences in litter material density, the mass of materials used to fill in the experimental surface varied (e.g., typical mass to fill in the chamber area was approximately 1 g cellulosic filter paper, 5 g basswood sheet, 3 g piñon pine needles, 2 g mesquite and grasses). We did not pretreat the litter materials to eliminate microbial activity, but experiments took place under conditions where materials were completely dry and were exposed to intense solar radiation, thus minimizing microbial activity (Johnson, 2003).

We analyzed the initial chemical composition characteristics of the litter materials using a solid state $^{13}C$-NMR CPMAS ($^{13}C$ nuclear magnetic resonance spectroscopy with cross-polarization and magic-angle spinning) with $^{1}H$ decoupling (Hatcher, 1987; Preston *et al.*, 1997). The NMR spectra were obtained using Bruker spectrometer (Bruker Instruments Inc., Karlsruhe, Germany) operating at 100 MHz for $^{13}C$. The samples were spun at 7.5 kHz. Prior to NMR analysis, litter was finely ground using a Cyclone Mill (UDY Corp., Fort Collins, CO, USA).

## Measurements

The rates of C-based trace gas production were quantified using a high resolution Wavelength-Scanned Cavity Ringdown Spectroscopy $CO_2$-$CH_4$-$H_2O$ analyzer (Model G2301, Picarro Inc., Santa Clara, CA, USA) and a reduced compound photometer CO-$H_2$ gas chromatograph (Peak Performer 1 RCP, Peak Laboratories LLC, Mountain View, CA, USA). A controlled flow of headspace gas (zero air or UHP grade $N_2$ at 50–70 mL min$^{-1}$) flowed through the chamber and the outlet was routed to the two analytical systems in sequence.

For the measurements of trace gas production in the presence of $O_2$, we used laboratory grade zero air. This provided sufficient amount of $O_2$ (~ 20% by volume) for photo-oxidation reactions. The zero air contained close to zero $CO_2$, but still contained atmospheric concentrations of other trace gases (e.g., 40 ppb CO and 2.88 ppm $CH_4$). The zero air was scrubbed of $CO_2$ and $H_2O$ prior to entering the chamber by passing it through a NaOH and Mg(ClO$_4$)$_2$ trap; measured $CO_2$ and $H_2O$ for the scrubbed air were not different from zero when measured using a $CO_2$-$CH_4$-$H_2O$ analyzer.

We conducted replicate measurement sets on the factorial combinations of chamber temperatures in the presence and the absence of simulated solar radiation. We consecutively increased the temperature by 10 °C from 15 °C to 55 °C with the chiller/heater for each set of measurements, cycling from +rad and −rad measurements at each temperature by covering the chamber with aluminum foil. Gas production responses to increased temperature and solar radiation exposure were instantaneous, but we waited approximately 30 min until gas concentrations stabilized. We then took sequential measurements over a 15 min poststabilization period (every 30 s for $CO_2$ and $CH_4$ and every 5 min for CO) and used the mean value of these measurements to establish the steady state production rate. Each measurement set was replicated four times for each litter type; means and standard errors were calculated from these replicates. For each measurement, trace gas concentrations were corrected with blank values obtained from exposing the empty chamber to the factorial combination of radiation and temperatures. In all cases, the blank values were below 5% of the values measured containing plant litter. The rate of trace gas production from thermal degradation of litter was estimated by quantifying the rate of gas production in the absence of solar radiation at a given temperature and subtracting gas production measured at 15 °C, when the gas production rates were near zero. To estimate the rate of trace gas production from photodegradation, we subtracted the rate of thermal degradation from the rate of total trace gas production in the presence of solar radiation at a given temperature.

For estimates of trace gas production from thermal degradation and photodegradation of basswood sheets in the absence of $O_2$, we followed the same procedure for measurements in the presence of $O_2$, except the measurements were taken at 15, 35, and 55 °C instead of every 10 °C. Ultra high purity $N_2$ was used for this experiment to eliminate $O_2$.

## Estimation of trace gas production from abiotic degradation of global plant litter

To demonstrate the applicability of our data, we combined our measurements with data from the literature to construct a rough estimate of global CO, $CO_2$, and $CH_4$ production rates from photodegradation of plant litter. An intensive extrapolation from laboratory CO production measurements suggests that 30–90 Tg CO yr$^{-1}$ is produced during photodegradation of plant litter globally (Schade & Crutzen, 1999; Schade *et al.*, 1999). We combined this estimated global flux with the ratios of $CO_2$, CO, and $CH_4$ quantified in our laboratory observations to estimate global production of $CO_2$ and $CH_4$ during abiotic decomposition of plant litter.

## Results

### *$^{13}$C-NMR analysis of plant material*

The $^{13}$C-NMR spectra and peak positions for the plant litter showed that the chemical compositions of the six plant materials used in our study were vastly different (Fig. 1; Table 1). Compared with the rest of the plant litter used, filter paper showed the simplest chemical composition; all the peak positions shown for filter paper represents *O*-alkyl group (45–110 ppm). In contrast, the other plant litter types exhibited peaks representing alkyl (0–45 ppm) and aromatic (110–165 ppm) groups as well as *O*-alkyl groups.

### *Trace gas production during abiotic degradation of plant litter*

We observed strong positive effects of temperature and solar radiation on the production of $CO_2$ and CO from all plant materials used (Fig. 2a–d). The $CO_2$ production rates were generally greater than CO, although the two gases were typically within an order of magnitude of each other at a given temperature (2.5–67.0 µmol $CO_2$ m$^{-2}$ hr$^{-1}$ and 1.8–34.1 µmol CO m$^{-2}$ hr$^{-1}$). Both $CO_2$ and CO production were highest in basswood sheet and lowest in filter paper. The $CH_4$ production rates (0.03–0.49 µmol $CH_4$ m$^{-2}$ hr$^{-1}$) responded positively to increased temperatures during thermal degradation of all materials (Fig. 2e), but only basswood clearly exhibited a temperature response in $CH_4$ production during photodegradation of plant litter (Fig. 2f).

### *The trace gas production during thermal degradation relative to photodegradation of plant litter*

The molar ratio between thermal degradation and photodegradation compares the relative importance of the two pathways within abiotic litter degradation. We found that the ratio of thermal degradation to photodegradation varied by gas species (Table 2). The thermal degradation to photodegradation ratio increased with temperature for all three gas species. The ratios of $CO_2$
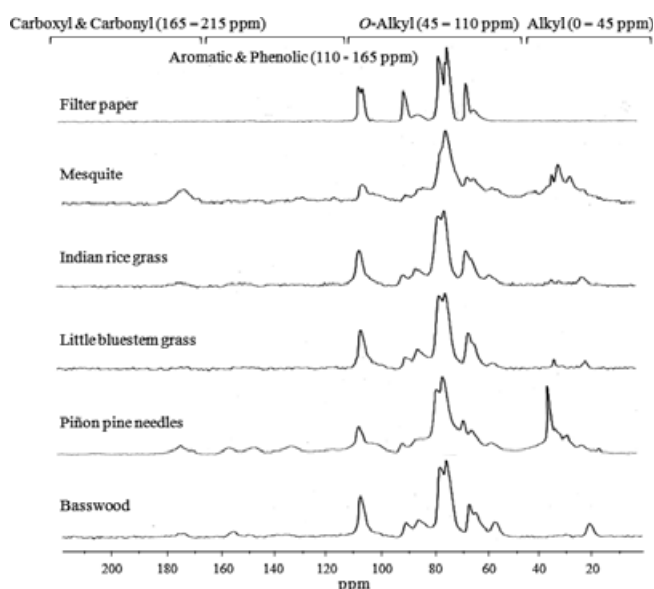


**Fig. 1** Solid state $^{13}$C-NMR CPMAS spectra of initial plant materials used in this study. The division and description of peaks is summarized in Table 1.

**Table 1** NMR peak positions for plant material and proximate-analysis fractions

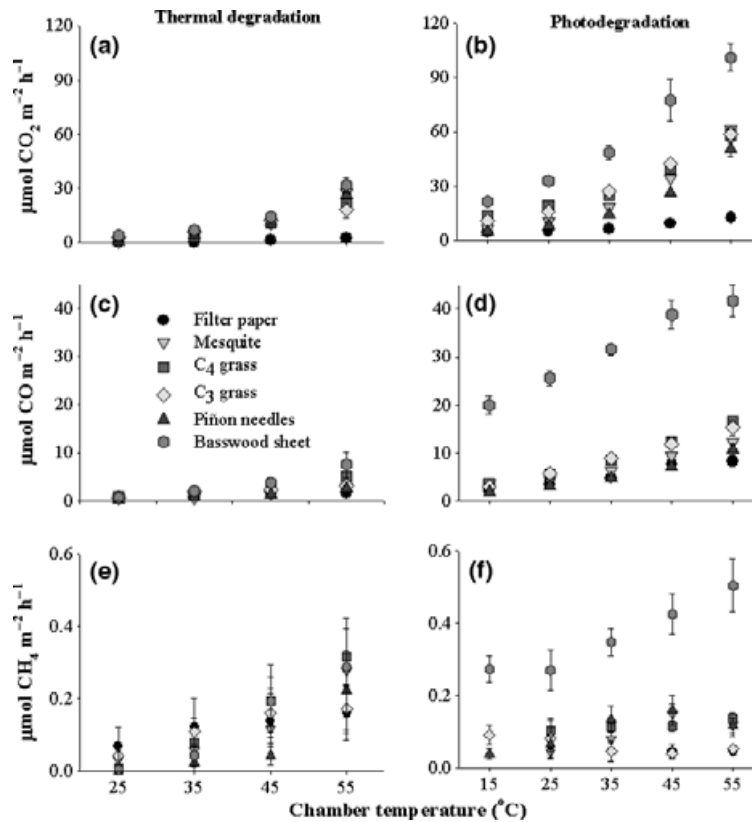| Plant material | Peak position (ppm) | | | | | | | | | | | | |
|---|---|---|---|---|---|---|---|---|---|---|---|---|---|
| Filter paper | 19 | | | | 58 | 69 | 87 | | 105 | | | | |
| Mesquite | 16 | | 28 | 37 | 55 | 68 | 81 | 101 | 105 | 117 | 132 | 150 | |
| C$_4$ grass | 14 | 22 | 31 | 41 | 58 | 69 | 86 | | 105 | 115 | 134 | 152 | 174 |
| C$_3$ grass | | 23 | | 33 | 56 | 70 | 86 | | 105 | 118 | 135 | 149 | 172 |
| Piñon needles | 16 | 24 | 32 | 40 | 50 | 67 | 84 | 101 | 105 | 113 | 133 | 150 | 170 |
| Basswood | 15 | 23 | 31 | | 55 | 69 | 86 | | 105 | 116 | 136 | 152 | 173 |

**Fig. 2** The rate of $CO_2$ (a and b), CO (c and d), and $CH_4$ (e and f) production from thermal degradation (a, c, and e) and photodegradation (b, d, and f) among the six plant litter types under changes in chamber temperature. Thermal degradation is the rate of gas production in the absence of solar radiation and photodegradation is the rate of gas production in the presence of solar radiation (total gas production) minus thermal degradation. Error bars indicate standard errors ($n = 4$).

production during thermal degradation to photodegradation ranged from 0.13 of total $CO_2$ produced at 25 °C to 0.59 at 55 °C (Table 2), which increased with temperature. Among the three gas species observed, CO showed the lowest thermal degradation to photodegradation ratio. The gases produced during photodegradation were greater than those produced during thermal degradation with the exception of $CH_4$ production at the highest temperature (thermal degradation to photodegradation ratio of 1.47 for $CH_4$ at 55 °C).

*The relative production of $CO_2$, CO, and $CH_4$ during abiotic degradation of plant litter*

The molar ratios of CO to $CO_2$ (hereafter 'CO: $CO_2$') were always below 0.6 and declined with increasing temperature (Fig. 3). This decline occurred for both thermal degradation and photodegradation (range = 0.35–1.00 at 15 °C and 0.25–0.52 at 55 °C, respectively) and for all materials used. The $CH_4$:$CO_2$ ratio also generally declined with temperature. Across the six materials used, the $CH_4$:$CO_2$ ratio was relatively

low (0.005–0.013) compared with the CO:$CO_2$ ratio; this was driven by low production rate of $CH_4$. In contrast to the CO:$CO_2$ ratio, the $CH_4$:$CO_2$ ratio from thermal degradation was greater than that from photodegradation (Fig. 3).

On average, $CO_2$ was the dominant gas species produced by both thermal degradation and photodegradation (Table 3); $CO_2$ contributed 62–80% of the total gas production during thermal degradation on a molar basis and approximately 70% during photodegradation. Changes in gas species contribution with temperature were more variable for thermal degradation than photodegradation (i.e., $CO_2$ contribution ranged from 63 to 80% from thermal degradation, but 67–72% from photodegradation of plant material).

*Trace gas production during abiotic degradation of plant litter in the absence of $O_2$*
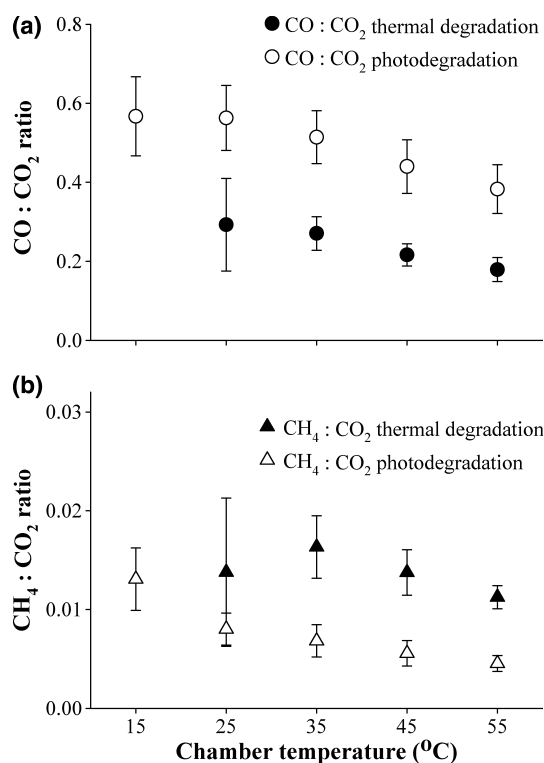
We observed surprisingly high rate of trace gas production during both thermal degradation and photodegradation of plant litter in the absence of $O_2$

**Table 2** The mean molar ratios between thermal degradation to photodegradation of $CO_2$, CO, and $CH_4$ across the six plant materials with increasing chamber temperatures (T)

| | Thermal degradation/Photodegradation | | |
| --- | --- | --- | --- |
| T (°C) | $CO_2$ | CO | $CH_4$ |
| 25 | 0.13 | 0.07 | 0.23 |
| 35 | 0.23 | 0.12 | 0.56 |
| 45 | 0.36 | 0.18 | 0.90 |
| 55 | 0.59 | 0.28 | 1.47 |

**Table 3** The molar % proportion of each gas from total C-based gas production during thermal degradation and photo-degradation of plant material under increasing chamber temperatures (T) Values in parentheses are standard errors ($n = 6$ plant materials)

| Abiotic process | T (°C) | $CO_2$ | CO | $CH_4$ |
| --- | --- | --- | --- | --- |
| Thermal degradation | 25 | 62.7 (13.4) | 34.7 (11.7) | 2.6 (1.8) |
| | 35 | 67.2 (13.4) | 29.5 (11.0) | 3.3 (2.4) |
| | 45 | 76.1 (7.6) | 22.3 (7.0) | 1.6 (0.6) |
| | 55 | 80.3 (5.0) | 18.3 (4.5) | 1.4 (0.5) |
| Photodegradation | 15 | 67.5 (4.1) | 31.5 (4.0) | 1.0 (0.2) |
| | 25 | 67.4 (3.3) | 32.1 (3.3) | 0.6 (0.1) |
| | 35 | 67.5 (2.9) | 32.0 (2.9) | 0.5 (0.1) |
| | 45 | 69.5 (3.0) | 30.0 (3.0) | 0.4 (0.1) |
| | 55 | 71.9 (2.9) | 27.8 (2.9) | 0.3 (0.0) |



**Fig. 3** The CO to $CO_2$ (a) and $CH_4$ to $CO_2$ (b) molar ratio from thermal degradation (open symbol) and photodegradation (closed symbol) of six plant materials under increasing chamber temperatures. Error bars indicate standard errors ($n = 6$ plant material).

*Estimated global $CO_2$, CO, and $CH_4$ production from abiotic degradation*

Combining our gas production ratio results at 25 °C (CO:$CO_2$ 0.56 and CO:$CH_4$ 70.19) with the estimated global CO production of 30–90 Tg CO yr$^{-1}$ during photodegradation of plant litter (Schade & Crutzen, 1999), we estimate global production of trace gases during photodegradation of plant litter to be 84–253 Tg $CO_2$ yr$^{-1}$ and 0.24–0.73 Tg $CH_4$ yr$^{-1}$. In addition, $CO_2$, CO, and $CH_4$ produced during thermal degradation would be 11–33 Tg $CO_2$ yr$^{-1}$, 2–6 Tg CO yr$^{-1}$, and 0.06–0.17 Tg $CH_4$ yr$^{-1}$, when using the gas production ratio of thermal degradation to pho-todegradation at 25 °C ($CO_2$ was 0.13, CO was 0.07, $CH_4$ was 0.23). Combining these values, the global abi-otic production of gases from plant litter would be roughly 95–286 Tg $CO_2$ yr$^{-1}$, 32–96 Tg CO yr$^{-1}$, and 0.30–0.90 Tg $CH_4$ yr$^{-1}$.

**Discussion**

Several studies in recent years have suggested that UV radiation plays an important role in degradation of plant litter and subsequent release of trace gases in arid ecosystems (Moorhead & Callaghan, 1994; Austin & Vivanco, 2006; Rutledge *et al.*, 2010). However, previous work on C-based trace gas production has been limited to single gas species and none has investigated the simultaneous production rates of the three major C-based trace gases ($CO_2$, CO, and $CH_4$) or their relative responses to temperature and solar radiation. Simultaneous measurements of these three gas species in the presence and absence of solar radiation (Fig. 2) and $O_2$ (Fig. 4) across a range of temperatures provided both important information about their relative contributions
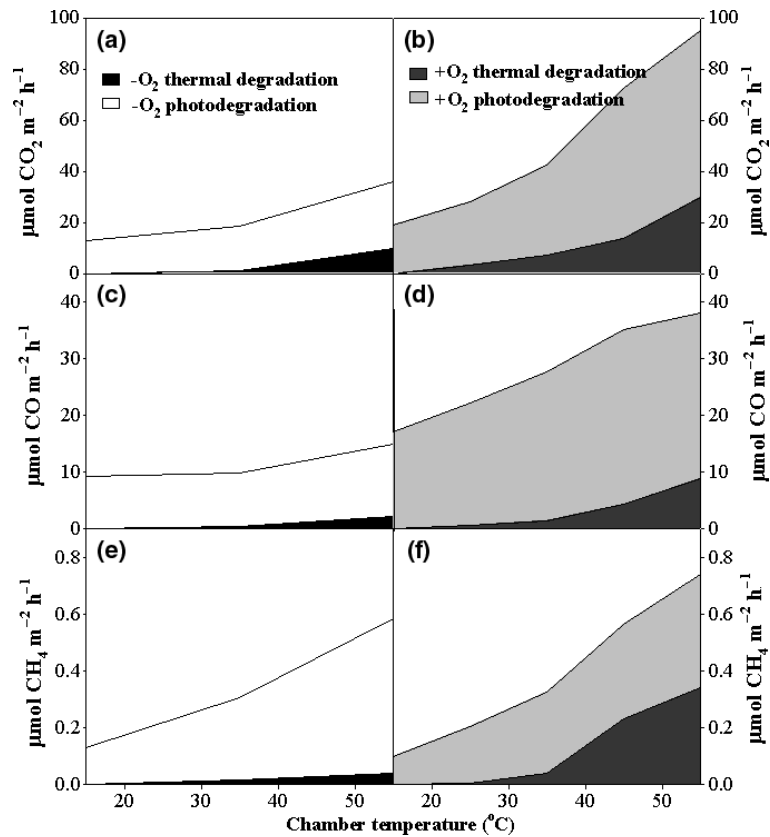
(Fig. 4). This pattern included even the oxidized gas forms, CO and $CO_2$. Under the same temperature and radiative conditions, $CO_2$ production in the absence of $O_2$ was 40–70% of that produced in the presence of $O_2$ (Fig. 4a and b). This pattern was similar in the case of CO (Fig. 4c and d), although relatively little CO was produced from thermal degradation in the absence of $O_2$. Interestingly, thermal production of $CH_4$ was even greater in the absence of $O_2$ compared with that in the presence of $O_2$ (Fig. 4e and f).

**Fig. 4** Production of $CO_2$ (a and b), CO (c and d), and $CH_4$ (e and f) from thermal degradation (darker) and photodegradation (lighter) of plant litter measured from basswood in the absence (a, c, and e) and presence of $O_2$ (b, d, and f).

to trace gas fluxes and also mechanistic insight into abiotic degradation of plant litter.

The variability in the rates and patterns of C-based trace gas release (Fig. 2) among the six plant materials used in our study suggests that the chemical composition of organic matter may be an important factor during abiotic litter decomposition. Several studies have reported significant chemical alteration of organic matter, in particular lignin, following solar or UV radiation exposure (Austin & Ballare, 2010; Feng *et al.*, 2011; Frouz *et al.*, 2011). Supporting this idea, basswood sheets showed the highest gas production rates for all three C-based gases (Fig. 2), whereas cellulosic filter paper, with simplest chemical structure (Fig. 1) showed the least (Fig. 2). The results did not change even when we exposed a thicker layer of cellulosic filter paper under solar radiation (data not shown), confirming that the rate of photodegradation was correlated to the area of exposure instead of mass as we expected (refer to 'Materials and methods'). The molecular composition of lignin provides numerous UV radiation absorption sites. When these sites absorb UV radiation, the chemical bonds excite to reactive levels and alter the chemical composition of lignin (Muller *et al.*, 2003; Luo *et al.*,

2009; Austin & Ballare, 2010). Although our data suggest that woody litter may produce substantial trace gases from abiotic litter degradation, additional studies with different wood types would help constrain the bounds of trace gas production estimates from lignin-dominated woody litter.

Measurable gas production from plant materials in the absence of solar radiation (Fig. 2) suggests that plant litter degrades via low temperature thermal degradation (< 100 °C) in the absence of microbially mediated decomposition processes. In contrast, soil microbial processes are known to consume CO and $CH_4$ under aerobic conditions (Conrad, 1996). In addition, substantial increases in both the $CO_2$ and CO production rates with temperatures above 35 °C provides additional evidence that the observed gas production was not microbially mediated, as the optimum temperature for typical microbial activity is reported as ~ 35 °C (Kirschbaum, 2010). A decrease in the $CO:CO_2$ ratio with temperature (Fig. 3) indicates that the $CO_2$ production may be more sensitive to temperature than CO, suggesting that the oxidative potential of this physicochemical process increases with temperature. Production of trace gases such as CO and $CH_4$ from plant

material in the absence of solar radiation has been reported previously (Conrad & Seiler, 1985; Tarr *et al.*, 1995; McLeod *et al.*, 2008), although the mechanism remains unknown. However, we speculate that trace gas release from plant materials in the absence of solar radiation may be due to thermal excitation of organic functional groups by lowering the barrier to reactivity with ROS or simple thermal decomposition. The thermal degradation process may be similar to photodegradation in the sense that chemical bonds forming organic matter may be excited to a reactive state, but differs in the specificity of bonds and potential reactive gas species involved. As incident solar radiative energy has greater potential energy than the thermal energy available at these temperatures, the rate of gas release per unit area of litter exposure would be expected to be lower for thermal degradation than photodegradation.

Significant, but slower rates of gas release during photodegradation of plant material in the absence of $O_2$ (Fig. 4) suggest that photo-oxidation utilizing atmospheric $O_2$ (Gao & Zepp, 1998) may be only one of several mechanisms driving photodegradation of plant litter as a whole. Release of CO during thermal degradation and photodegradation of litter in the absence of $O_2$ was reported previously (Tarr *et al.*, 1995); however, production of $CO_2$ (Fig. 4a and b), the most oxidized of the three species, was particularly notable in our study. Our results suggest that there may be multiple mechanisms involved in the release of C-based trace gases during abiotic litter degradation: those that require $O_2$ and those that operate in the absence of $O_2$ (Fig. 5). We speculate that solar radiative energy breaks the chemical bonds of carboxyl (R-COO-) or carbonyl (R-CO-) groups (Fig. 5a) and directly produces $CO_2$ and CO without an oxidizing process. Alternatively, we speculate that $O_2$ present within plant cell and carbon compounds may have been used (Crestini & Dauria, 1996) during photodegradation of litter in the absence of atmospheric $O_2$. Simultaneously, reactive functional groups can be oxidized by $O_2$ or other ROS in the atmosphere and produce $CO_2$ and CO (Fig. 5b). This process is widely known as photo-oxidation because the photochemical reaction is mediated by free oxidized species in the atmosphere. Similarly, the higher rate of $CH_4$ released in the absence of $O_2$ suggests that in the presence of $O_2$, a portion of $CH_4$ released may instantaneously be oxidized to become $CO_2$ or CO via photo-oxidation processes.

Current global change projections suggest that the importance of abiotic decomposition processes to the global C cycle may increase in the future. The positive relationship between trace gas production and temperature (Fig. 2) suggests that abiotic degradation of plant litter will increase in accordance with projected increases in global atmospheric temperature. Although we hypothesized that thermal and photodegradation should obey a normal exponential increase with respect to temperature, we recognize that these are processes that may have additional dependencies related to material properties (e.g., activated functional groups). Increases in aridity in certain regions (IPCC, 2007) may also further enhance the relative importance of abiotic decomposition by decreasing the rates of microbially mediated decomposition. Although this study did not address the effects of radiation intensity on photodegradation, other studies have suggested that future increases in the intensity of UV radiation reaching the Earth's surface (Cheymol & De Backer, 2003) may stimulate the rate of litter photodegradation and trace gas release (Schade *et al.*, 1999; McLeod *et al.*, 2008; Rutledge *et al.*, 2010). An increase in the proportion of woody litter into arid and semi-arid ecosystems due to woody encroachment (Archer *et al.*, 2001) may result in greater trace gas release as a result of abiotic degradation, as we observed basswood had the highest rates of trace gas production and was the most sensitive to increasing temperatures. Ecologically, enhanced abiotic litter decomposition may also accelerate microbial decomposition as chemical composition of stable compounds such as lignin can be significantly altered to facilitate microbial attack (Gallo *et al.*, 2009; Foereid *et al.*, 2010), further shifting the importance of abiotic and biotic decomposition processes under a changing climate.

We suggest that (1) the abiotic degradation rate of plant litter varies with different chemical compounds present in plant litter, (2) the rate of abiotic litter decomposition is positively correlated with temperature, (3) low temperature thermal degradation of plant litter occurs via physico-chemical breakdown of chemical bonds and this process increases with temperature even in the absence of solar radiation, and (4) photo-oxidation process occurs with solar radiation exposure, but photo-oxidation is only a part of photochemical
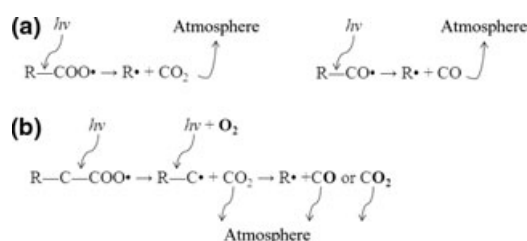


**Fig. 5** Two potential mechanisms of $CO_2$ and CO release during photodegradation of plant litter: a) physical breakdown of carboxyl (R-COO-) and carbonyl (R-CO-) group by solar radiation energy and b) photochemically mediated oxidation (photo-oxidation). The '*hv*' represents incident solar radiation.

breakdown of plant litter. Our rough estimation of global abiotic production of $CO_2$, CO, and $CH_4$ suggests that approximately 40–105 Tg C $yr^{-1}$ (26–78 Tg $CO_2$-C $yr^{-1}$, 14–26 Tg CO-C $yr^{-1}$, and 0.2–0.7 Tg $CH_4$-C $yr^{-1}$) may be released from abiotic degradation of plant litter. In the context of global C cycling, our estimation of C release during abiotic decomposition of plant litter is small (e.g., global flux of C from soil respiration is approximately 75 Pg C $yr^{-1}$, fossil fuel burning is 5 Pg C $yr^{-1}$, land use change is 1–2 Pg C $yr^{-1}$, and gross primary production is 100 Pg C $yr^{-1}$ (Canadell et al., 2007; Raich & Potter, 1995; Schlesinger & Andrews, 2000). However, our study supports the concept that abiotic decomposition of organic material may contribute to global C fluxes as a noticeable and currently is under accounted, for source of C.

## Acknowledgements

## References

Archer S, Boutton T, Hibbard K (2001) Trees in grasslands: biogeochemical consequences of woody plant expansion. In: Global Biogeochemical Cycles in the Climate System (eds Schultz E, Harrison S, Heiman M et al.), pp. 115–138. Academic Press, San Diego.

Arola A, Koskela T (2004) On the sources of bias in aerosol optical depth retrieval in the UV range. Journal of Geophysical Research-Atmospheres, 109, D08209, doi: 10.1029/2003JD004375.

Austin AT (2011) Has water limited our imagination for aridland biogeochemistry? Trends in Ecology & Evolution, 26, 229–235.

Austin AT, Ballare CL (2010) Dual role of lignin in plant litter decomposition in terrestrial ecosystems. Proceedings of the National Academy of Sciences of the United States of America, 107, 4618–4622.

Austin AT, Vivanco L (2006) Plant litter decomposition in a semi-arid ecosystem controlled by photodegradation. Nature, 442, 555–558.

Brandt LA, King JY, Milchunas DG (2007) Effects of ultraviolet radiation on litter decomposition depend on precipitation and litter chemistry in a shortgrass steppe ecosystem. Global Change Biology, 13, 2193–2205.

Brandt LA, Bohnet C, King JY (2009) Photochemically induced carbon dioxide production as a mechanism for carbon loss from plant litter in arid ecosystems. Journal of Geophysical Research-Biogeosciences, 114, G02004, doi: 10.1029/2008JG000772.

Brandt LA, King JY, Hobbie SE, Milchunas DG, Sinsabaugh RL (2010) The role of photodegradation in surface litter decomposition across a grassland ecosystem precipitation gradient. Ecosystems, 13, 765–781.

Bruhn D, Mikkelsen TN, Obro J, Willats WGT, Ambus P (2009) Effects of temperature, ultraviolet radiation and pectin methyl esterase on aerobic methane release from plant material. Plant Biology, 11, 43–48.

Caldwell MM, Bornman JF, Ballare CL, Flint SD, Kulandaivelu G (2007) Terrestrial ecosystems, increased solar ultraviolet radiation, and interactions with bother climate change factors. Photochemical & Photobiological Sciences, 6, 252–266.

Canadell JG, Le Quere C, Raupach MR et al. (2007) Contributions to accelerating atmospheric $CO_2$ growth from economic activity, carbon intensity, and efficiency of natural sinks. Proceedings of the National Academy of Sciences of the United States of America, 104, 18866–18870.

Cheymol A, De Backer H (2003) Retrieval of the aerosol optical depth in the UV-B at Uccle from Brewer ozone measurements over a long time period 1984–2002. Journal of Geophysical Research-Atmospheres, 108, 4800, doi: 10.1029/2003JD003758.

Conrad R (1996) Soil microorganisms as controllers of atmospheric trace gases ($H_2$, CO, $CH_4$, OCS, $N_2O$, and NO). Microbiological Reviews, 60, 609–640.

Conrad R, Seiler W (1985) Influence of temperature, moisture, and organic carbon on the flux of $H_2$ and CO between soil and atmosphere – Field studies in sub-tropical regions. Journal of Geophysical Research-Atmospheres, 90, 5699–5709.

Crestini C, Dauria M (1996) Photodegradation of lignin: the role of singlet oxygen. Journal of Photochemistry and Photobiology a-Chemistry, 101, 69–73.

Day TA, Zhang ET, Ruhland CT (2007) Exposure to solar UV-B radiation accelerates mass and lignin loss of Larrea tridentata litter in the Sonoran Desert. Plant Ecology, 193, 185–194.

DeFries RS, Townshend JRG (1994) NDVI-derived land-cover classifications at a global-scale. International Journal of Remote Sensing, 15, 3567–3586.

Feng X, Hills KM, Simpson AJ, Whalen JK, Simpson MJ (2011) The role of biodegradation and photo-oxidation in the transformation of terrigenous organic matter. Organic Geochemistry, 42, 262–274.

Foereid B, Bellarby J, Meier-Augenstein W, Kemp H (2010) Does light exposure make plant litter more degradable? Plant and Soil, 333, 275–285.

Frouz J, Cajthaml T, Mudrák O (2011) The effect of lignin photodegradation on decomposability of Calamagrostis epigeios grass litter. Biodegradation, 22, 1247–1254.

Gallo ME, Porras-Alfaro A, Odenbach KJ, Sinsabaugh RL (2009) Photoacceleration of plant litter decomposition in an arid environment. Soil Biology & Biochemistry, 41, 1433–1441.

Gao HZ, Zepp RG (1998) Factors influencing photoreactions of dissolved organic matter in a coastal river of the southeastern United States. Environmental Science & Technology, 32, 2940–2946.

Gholz HL, Wedin DA, Smitherman SM, Harmon ME, Parton WJ (2000) Long-term dynamics of pine and hardwood litter in contrasting environments: toward a global model of decomposition. Global Change Biology, 6, 751–765.

Hatcher PG (1987) Chemical structural studies of natural lignin by dipolar dephasing solid-state C-13 nuclear-magnetic-resonance. Organic Geochemistry, 11, 31–39.

Henry HAL, Brizgys K, Field CB (2008) Litter decomposition in a california annual grassland: interactions between photodegradation and litter layer thickness. Ecosystems, 11, 545–554.

IPCC (2007) Climate Change 2007: The Physical Science Basis. Cambridge University Press, Cambridge, United Kingdom.

Jobbagy EG, Jackson RB (2000) The vertical distribution of soil organic carbon and its relation to climate and vegetation. Ecological Applications, 10, 423–436.

Johnson D (2003) Response of terrestrial microorganisms to ultraviolet-B radiation in ecosystems. Research in Microbiology, 154, 315–320.

Keppler F, Hamilton JTG, McRoberts WC, Vigano I, Brass M, Rockmann T (2008) Methoxyl groups of plant pectin as a precursor of atmospheric methane: evidence from deuterium labelling studies. New Phytologist, 178, 808–814.

Kirschbaum MUF (2010) The temperature dependence of organic matter decomposition: seasonal temperature variations turn a sharp short-term temperature response into a more moderate annually averaged response. Global Change Biology, 16, 2117–2129.

Luo X, Zhan H, Chai X-S, Fu S, Liu J (2009) A novel method for determination of aromatic aldehyde monomers in lignin degradation liquor. Industrial & Engineering Chemistry Research, 48, 2713–2716.

Matthews E (1997) Global litter production, pools, and turnover times: estimates from measurement data and regression models. Journal of Geophysical Research-Atmospheres, 102, 18771–18800.

McCalley CK, Sparks JP (2009) Abiotic gas formation drives nitrogen loss from a desert ecosystem. Science, 326, 837–840.

McLeod AR, Fry SC, Loake GJ, Messenger DJ, Reay DS, Smith KA, Yun BW (2008) Ultraviolet radiation drives methane emissions from terrestrial plant pectins. New Phytologist, 180, 124–132.

Moorhead DL, Callaghan T (1994) Effects of increasing ultraviolet-B radiation on decomposition and soil organic-matter dynamics – a synthesis and modeling study. Biology and Fertility of Soils, 18, 19–26.

Muller U, Ratzsch M, Schwanninger M, Steiner M, Zobl H (2003) Yellowing and IR-changes of spruce wood as result of UV-irradiation. Journal of Photochemistry and Photobiology B-Biology, 69, 97–105.

Pancotto VA, Sala OE, Robson TM, Caldwell MM, Scopel AL (2005) Direct and indirect effects of solar ultraviolet-B radiation on long-term decomposition. Global Change Biology, 11, 1982–1989.

Preston CM, Trofymow JA, Sayer BG, Niu JN (1997) C-13 nuclear magnetic resonance spectroscopy with cross-polarization and magic-angle spinning investigation of the proximate-analysis fractions used to assess litter quality in decomposition studies. Canadian Journal of Botany-Revue Canadienne De Botanique, 75, 1601–1613.

Raich JW, Potter CS (1995) Global patterns of carbon-dioxide emissions from soils. *Global Biogeochemical Cycles*, **9**, 23–36.

Rosentreter R, Belnap J (2003) Biological soil crusts of North America. In: *Biological Soil Crusts: Structure, Function, and Management* (eds Belnap J, Lange OL), pp. 31–50. Springer-Verlag, Berlin.

Rozema J, Tosserams M, Nelissen HJM, vanHeerwaarden L, Broekman RA, Flierman N (1997) Stratospheric ozone reduction and ecosystem processes: enhanced UV-B radiation affects chemical quality and decomposition of leaves of the dune grassland species *Calamagrostis epigeios*. *Plant Ecology*, **128**, 284–294.

Rutledge S, Campbell DI, Baldocchi D, Schipper LA (2010) Photodegradation leads to increased carbon dioxide losses from terrestrial organic matter. *Global Change Biology*, **16**, 3065–3074.

Schade GW, Crutzen PJ (1999) CO emissions from degrading plant matter (II). Estimate of a global source strength. *Tellus Series B-Chemical and Physical Meteorology*, **51**, 909–918.

Schade GW, Hofmann RM, Crutzen PJ (1999) CO emissions from degrading plant matter (I). Measurements. *Tellus Series B-Chemical and Physical Meteorology*, **51**, 889–908.

Schlesinger WH, Andrews JA (2000) Soil respiration and the global carbon cycle. *Biogeochemistry*, **48**, 7–20.

Tarr MA, Miller WL, Zepp RG (1995) Direct carbon-monoxide photoproduction from plant matter. *Journal of Geophysical Research-Atmospheres*, **100**, 11403–11413.

Throop HL, Archer SR (2007) Interrelationships among shrub encroachment, land management, and litter decomposition in a semidesert grassland. *Ecological Applications*, **17**, 1809–1823.

Throop HL, Archer SR (2009) Resolving the dryland decomposition conundrum: some new perspectives on potential drivers. *Progress in Botany*, **70**, 171–194.

Uselman SM, Snyder KA, Blank RR, Jones TJ (2011) UVB exposure does not accelerate rates of litter decomposition in a semi-arid riparian ecosystem. *Soil Biology & Biochemistry*, **43**, 1254–1265.

Valentine RL, Zepp RG (1993) Formation of carbon-monoxide from the photodegradation of terrestrial dissolved oganic-carbon in natural-waters. *Environmental Science & Technology*, **27**, 409–412.

Vigano I, van Weelden H, Holzinger R, Keppler F, McLeod A, Rockmann T (2008) Effect of UV radiation and temperature on the emission of methane from plant biomass and structural components. *Biogeosciences*, **5**, 937–947.

Vigano I, Rockmann T, Holzinger R *et al.* (2009) The stable isotope signature of methane emitted from plant material under UV irradiation. *Atmospheric Environment*, **43**, 5637–5646.